

Image Separation vs. Redshift of Lensed QSOs: Implications for Galaxy Mass Profiles

Liliya L. R. Williams^{*}

Institute of Astronomy, Madingley Road, Cambridge, CB3 0HA

Accepted for publication in MNRAS

ABSTRACT

Recently, Park and Gott reported an interesting observation: image separation of lensed QSOs declines with QSO redshift more precipitously than expected in any realistic world model, if the lenses are taken to be either singular isothermal spheres or point masses. In this Letter I propose that the observed trend arises naturally if the lensing galaxies have logarithmic surface mass density profiles that gradually change with radius. If the observed lack of central (odd) images is also taken into account, the data favor a universal dark matter density profile over an isothermal sphere with a core. Since the trend of image separation vs. source redshift is mostly a reflection of galaxy properties, it cannot be straightforwardly used as a test of cosmological models. Furthermore, the current upper limits on the cosmological constant may have to be revised.

Key words: gravitational lensing – cosmology – galaxies: structure

1 INTRODUCTION

Since gravitational lensing takes place over cosmological distances, it can in principle be used to measure cosmological parameters, such as mass density, Ω , and cosmological constant, Λ . For example, the frequency of multiply imaged QSOs is a sensitive function of Λ , and therefore the observed abundance of lensed QSOs has been used to place upper limits on Λ (Turner 1990; Fukugita et al. 1992; Kochanek 1996). Another example is the relation between image separation, θ_{im} and source redshift, z_s of multiply split QSOs, which mostly depends on the sum of Ω and Λ , and thus should serve as a good indicator of the curvature of the Universe. (Gott, Park & Lee 1989; Fukugita et al. 1992, Park & Gott 1997, hereafter PG97). If the Universe is flat and galaxies are singular isothermal spheres, the $\theta_{im}-z_s$ relation should be flat, i.e. independent of source redshift. If the Universe is open, there should be a mild decline of image separations with redshift; a $\sim 20\%$ decline is expected between $z_s \sim 1.5$ and 5, in an extreme $\Omega = 0$ case.

The mildness of the expected $\theta_{im}-z_s$ trend can be explained as follows. For any given lens, and fixed lens and source redshifts the image separation of images with comparable brightness is quite independent of source impact parameter. Since optimal lens redshift for any high redshift source is roughly the same, $z_l \sim 0.5$, and angular diameter distances vary little past $z \sim 0.5$, the observed image separation should change little with z_s . If a population of

lenses is considered, having a range of properties, like scale lengths and velocity dispersions, there will be a corresponding spread in image separations, but still little or no trend with z_s .

Yet the observed θ_{im} of lensed QSOs declines strongly with z_s (See Figure 1 of PG97, or Figure 2 of this paper.) PG97 present a list of source redshifts and image separations of 20 multiply imaged QSOs. The source redshifts span a range between 1.4 and 4.5, and image separation between $0.5''$ and $7''$. There is a drop of at least a factor of 4 in image separation from the low- z_s to high- z_s cases. According to PG97, in a flat Universe such distribution can be ruled out at 99% confidence level, while in the most extreme empty Universe, it is ruled out at 97%. To make the confidence level decrease below 95%, one would need to ‘remove’ 2–3 largest separation or highest redshift cases from the sample. (See PG97 for a discussion of statistical significance, possible errors, etc.)

In this Letter, I suggest that the trend, which is due to the lack of high redshift wide separation lensed QSOs is naturally reproduced if a set of three conditions is met, (i) galaxies’ central mass profiles have logarithmic slopes that change with radius, (ii) there is a dispersion in galaxy properties, like central surface mass densities or velocity dispersion, and (iii) the characteristic length scale of galaxy dark matter halos varies with galaxy luminosity as $r \propto L^a$, where $0 < a \lesssim 0.5$.

^{*} Email: llrw@ast.cam.ac.uk

2 MODEL

In this section I describe the lensing model, and introduce some simplifying assumptions about the lenses, galaxies, and sources, QSOs. I do not aim to produce a detailed model because the small number of lensed QSOs in the current sample does not necessitate it. I need not assume any particular cosmological model, because the effect implied by the present model is considerably stronger than that of cosmology.

2.1 Model Assumptions

2.1.1 Lenses

I consider two types of galaxy mass profile, an isothermal sphere with a core, ISC, and a universal dark matter profile, NFW, derived from numerical simulations of Navarro, Frenk & White (1995, 1996). These profiles were chosen because their logarithmic surface mass density gradually flattens with decreasing radius. The reason for using these, as opposed to constant power law profiles, like a singular isothermal sphere, is discussed in Section 3. Both ISC and NFW provide a plausible description of the dark matter halos of galaxies. ISC is commonly used because of the observed shapes of the rotation curves of spiral galaxies. Additionally, based on the results of the HST Snapshot Survey, Maoz & Rix (1993, hereafter MR93) conclude that ellipticals must possess ISC-type dark matter halos in order to reproduce the observed image separation distribution of multiply imaged QSOs. The NFW profile has been recently claimed as a universal dark matter halo profile describing halos of gravitationally bound structures over 4 orders of magnitude in mass. It is also supported on theoretical grounds (Evans & Collett 1997). I assume that all galaxy-lenses are circularly symmetric.

A description of the lensing properties of these profiles can be found in Schneider et al. (1992), Bartelmann (1996), and Williams & Lewis (1997). It suffices to say here that ISC is roughly flat within core radius r_c , and has an isothermal density profile outside. The vertical normalization of the profile is fixed by its central surface mass density, κ_0 , in terms of critical density for lensing, Σ_{crit} . NFW is singular at the centre, its logarithmic slope gradually steepens from $\rho \propto r^{-1}$ at the centre, to $\rho \propto r^{-3}$ at large radii, and is isothermal around the characteristic scale length, r_s . The vertical normalization of its projected surface mass density is proportional to κ_s , which is given in terms of Σ_{crit} .

As was pointed out by PG97, the scatter in the observed θ_{im-z_s} points is large. One of the main sources of scatter is probably the spread in galaxy-lens properties. For example, a singular isothermal sphere lens of a given σ_v produces a constant bending angle at the lens, and hence image separation varies as D_{ls}/D_{os} , where the D 's are the lens-source and observer-source angular diameter distances. If all lensing galaxies had the same σ_v , one would expect the observed angular image separations to be proportional to the corresponding D_{ls}/D_{os} values, whereas a plot of D_{ls}/D_{os} vs. θ_{im} , in 8 systems where both z_s and z_l are known reveals no correlation at all, and a scatter in θ_{im} of a factor of a few larger than the scatter in D_{ls}/D_{os} . This strongly suggests that the spread in galaxy-lens properties is important. Therefore I assume a *family* of galaxy-lenses, each having the same scale length, r_c and r_s for ISC and NFW respectively, but a range

of κ_0 and κ_s , which is equivalent to a range in velocity dispersions.

I assume that r_c and r_s and galaxy luminosity function do not evolve with redshift, at least in the interval most relevant here, i.e. optimal lens redshift for high- z sources, $z_l \sim 0.3 - 1$. This assumption is supported by the recent spectroscopic observations of Lilly et al. (1995), which indicate that the luminosity function of elliptical galaxies, i.e. the galaxy population that is believed to provide the bulk of the lensing optical depth (see MR93), evolves very little from $z \sim 1$ to the present.

When the source impact parameter is sufficiently small, all the NFW lenses, and ISC lenses with $\kappa_0 > 1$ produce 3 images, whereas the observed multiply imaged systems mostly have an even number of images, either 2 or 4. This is thought to be because the central (odd) image is demagnified below visibility. I will return to the importance of the central odd image later, in Section 2.2. The circularly symmetric lenses considered here cannot produce 5 image systems; observed 4(+1) cases are a property of elliptical lenses. However the present treatment will not suffer if only symmetric lenses are considered.

For sources at large redshifts, the optimal lens redshift increases very slowly with z_s in all cosmologies except for the most extreme Λ dominated cases. So I will assume that z_l is constant, independent of z_s . The critical surface mass density for lensing, Σ_{crit} changes little with z_s , if z_l is fixed, and sources are at high z_s . For example, in an $\Omega=0.3$ open Universe, moving the source from $z_s=1$ to 5 reduces Σ_{crit} by 17%, if $z_l = 0.2$. Therefore, I will assume that galaxy-lens projected surface mass density is given by κ_0 and κ_s , with no dependence on redshifts.

2.1.2 Sources

Analytic fits to QSO luminosity function (QLF) usually take the form of a double power law, with steep bright-end slope and shallow faint-end slope; the transition occurs at some characteristic luminosity, L_0 , which evolves with redshift, and is commonly parameterized as $L_0(z_s) \propto (1+z_s)^\alpha$. Boyle et al. (1990) derive a pure luminosity evolution for $z \lesssim 2$ QSOs, with $\alpha=3.2$, while Hewett et al. (1993) conclude that QLF changes shape with redshift, and that evolution must slow down beyond $z \sim 1.5$ compared to the predictions of Boyle et al. For $2 \lesssim z \lesssim 3$ they derive $\alpha \sim 1.5$. QSO evolution at higher redshifts, up to 5 is less constrained, though it is sometimes assumed that the shape of the QLF does not evolve beyond $z \sim 2$, while L_0 evolves such that it 'slides' brightward along the high luminosity part of the QLF (Wallington & Narayan 1993). I assume that at any given redshift there are no QSOs brighter than L_0 , and that QLF at $L < L_0$ is $N_{QSO}(L) \propto L^{-s}$, with $s = 1.2$ (MR93). I adopt the α parameterization of QSO evolution for high redshifts, and derive results for $\alpha=0$, and 2.

2.2 Results

We are interested in two lensing properties of the galaxy-lenses: image separation and total image magnification. Given a galaxy-lens, a source can have a range of impact parameters, each resulting in a different image magnification, and image separation, even though the latter tends to

stay rather constant, roughly equal to twice the Einstein ring radius of the lens. To account for a range of source impact parameters, I calculate the impact parameter weighted averages of image magnification, $\langle \mu \rangle$ and image separation, $\langle \theta \rangle$ as a function of κ_0 or κ_s , for ISC and NFW respectively.

Figure 1 shows the results. Vertical normalization of image separation is irrelevant for now. The important feature is that for both profiles the image separation increases with κ_0 or κ_s , while total image magnification decreases. In other words, given a population of galaxy-lenses with a range of κ_0 or κ_s , image magnification goes inversely with image separation. Now, image magnification couples to source redshift, as follows. Flux of an L_0 QSO is given by,

$$\begin{aligned} f &\propto \mu(z_s)L_0(z_s)/D_L(z_s)^2 \\ &\propto \mu(z_s)(1+z_s)^\alpha/D_A(z_s)^2(1+z_s)^4 \\ &\propto \mu(z_s)(1+z_s)^{\alpha-4}, \end{aligned} \quad (1)$$

where $\mu(z_s)$ is total image magnification, and D_L and D_A are the luminosity and angular diameter distances respectively. In the second and third lines I used the fact that $D_L = (1+z)^2 D_A \propto (1+z)^2$, since angular diameter distance stays roughly constant for high- z_s sources. So to make it into a magnitude limited sample, with a certain f_{lim} , an L_0 QSO at z_s has to be magnified by at least

$$\mu(z_s) \propto f_{lim}(1+z_s)^{4-\alpha}, \quad (2)$$

with fainter QSOs magnified more. Because larger redshift QSOs undergo larger magnifications, a fixed f_{lim} of any given survey translates into a lower limit on $\langle \mu \rangle$ as a function of z_s , which in turn implies an upper limit on $\langle \theta \rangle$, as read off from Figure 1. The resulting relation is plotted as solid (ISC) and dashed (NFW) curves in Figure 2, for two values of QSO luminosity function evolution parameters, α ; 0, and 2. Both sets of curves reproduce the upper envelope of the observed points quite well. The paucity of observed points does not allow to differentiate between α of 0 and 2, or between ISC and NFW profiles.

The curves are scaled vertically and horizontally to roughly match the observed distribution. Adjusting the scaling in the vertical direction yields the angular size of r_c and r_s respectively. For ISC angular core radius is $0.37''$, while for NFW angular scale radius is $1.25''$. For typical lens redshifts of 0.5 these translate into $r_c = 1.4h^{-1}$ kpc, and $r_s = 4.6h^{-1}$ kpc. These values are roughly what one would derive from modelling individual multiple-image systems using ISC/NFW profiles. Scaling the curves in the horizontal direction gives the average *minimum* magnification of lensed QSOs as a function of z_s . For $\alpha = 0$ models, $\langle \mu \rangle/f_{lim} = 0.039(1+z_s)^4$, and for $\alpha = 2$, $\langle \mu \rangle/f_{lim} = 0.4(1+z_s)^2$; i.e. if QSO characteristic luminosity does not evolve, a lower limit on magnification of QSOs at $z = 3$ is $\langle \mu \rangle/f_{lim} = 10$, whereas it is 6.4 if $L_0(z_s) \propto (1+z_s)^2$. Surveys with brighter f_{lim} have higher $\langle \mu \rangle$, but the dependence on $(1+z_s)$ is weak, and most existing surveys have f_{lim} of 1–2 magnitudes within each other.

Let us summarize the conclusions thus far. Roughly, Figure 1 implies that average image magnification is inversely proportional to the galaxy central surface mass density, $\langle \mu \rangle \propto \kappa_{0,s}^{-1}$; and that average image separation is directly proportional to the galaxy central surface mass density, $\langle \theta \rangle \propto \kappa_{0,s}$. In general, the observed image separation is also proportional to the characteristic scale length of the

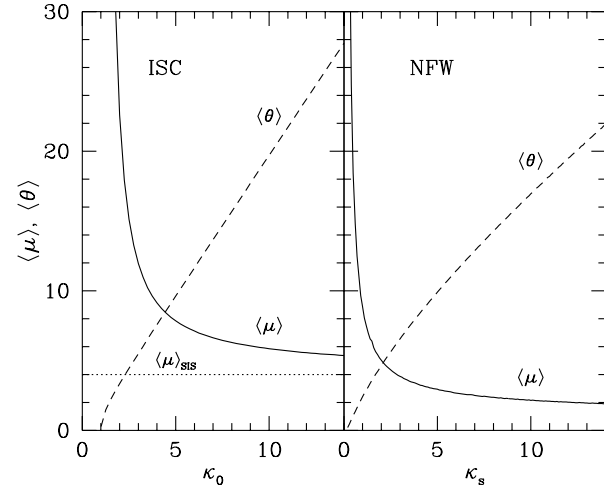


Figure 1. Magnification and image separation vs. the central surface density of two different types of lenses: ISC and NFW. Both magnification and image separation are impact parameter weighted averages of these quantities. The dotted line is the impact parameter weighted average magnification of a singular isothermal sphere. Note that for ISC and NFW profiles the magnification and image separation go in the opposite sense with increasing κ_0 and κ_s , while for SIS the average magnification is always a constant (see Section 3).

galaxy-lens, so $\langle \theta \rangle \propto \kappa_{0,s} r_{c,s}$, but since I have so far assumed that all galaxies have the same characteristic scale length, I have not used the latter dependence. The scale length can be a function of central concentration, $r_c \propto \kappa_{0,s}^{\beta}$. Combining these relations gives, $\langle \mu \rangle \propto \langle \theta \rangle^{-\frac{1}{1+\beta}}$, and together with eq.(2) it implies,

$$\langle \theta \rangle \propto (1+z_s)^{-(1+\beta)(4-\alpha)} \quad (3).$$

With $\beta = 0$ this equation basically reproduces the curves in Figure 2. Note that β does not have to be 0, any value between roughly -0.5 and 2 will do, i.e. the total exponent in eq. (3) should be around *-few*. I will return to the discussion of β and its implications for the dark matter halos of galaxies in Section 4.

Thus both ISC and NFW galaxy-lens models can reproduce the observed $\theta_{im}-z_s$ trend, and neither is preferred based on these observations alone. However, another widely documented observation can break the tie; all multiply imaged QSOs lack the central odd-numbered image, i.e. observed cases are either doubles or quadruples. This has long been interpreted as evidence in favor of centrally condensed galaxy profiles, which would demagnify the central image below visibility. The other possible explanation, dust obscuration in the centres of galaxies, is largely ruled out because radio observations of multiply split QSOs also do not reveal central images (Myers et al. 1995). I apply this argument here: ISC model predicts that $\kappa_0 \sim 1 - 2$ models should have central images of brightnesses comparable to the primary image, while with the NFW models the central images of low κ_s lenses should be 5-10 times demagnified compared

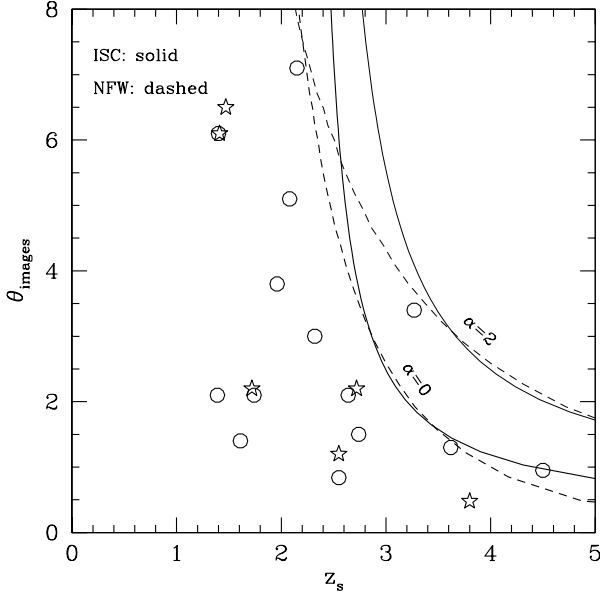


Figure 2. Image separation vs. source redshift. The points are the observed multiply imaged QSOs (taken from Table 1 of PG97); stars represent the lenses from the HST Snapshot Survey (MR93), circles are from other, ground based surveys. Predictions of the isothermal sphere with a core, ISC and universal dark matter halo, NFW models (labeled) were normalized vertically and horizontally, as described in Section 2.2. Both ISC and NFW profiles can account for the observed trend.

to the primary image. This rules strongly in favor of the NFW model.

3 IMPLICATIONS FOR GALAXY MASS PROFILES

The key feature of the galaxy lens population that allows to reproduce the envelope is that image separation goes inversely with image magnification. This allows magnification bias, which acts through image magnification, to couple image separation to source redshift. This property of a lens population is a direct consequence of the individual galaxies having a changing logarithmic slope, as in the ISC and NFW models. Lenses that do not have this property, for example singular isothermal spheres and point masses, cannot reproduce the observed envelope.

For a singular isothermal sphere (SIS) the average impact parameter weighted magnification can be calculated to be 4, independent of the velocity dispersion, σ_v , while image separation is proportional to σ_v^2 . So $\langle\mu\rangle$, being a ‘universal’ constant, does not couple to $\langle\theta\rangle$, and thus SIS cannot reproduce the observed trend. The property that $\langle\mu\rangle$ is constant is not unique to SIS, but can be generalized to any family of mass profiles with no in-built scale length, like single power-laws and point masses. In such models the only parameter is the absolute mass normalization of the profile, which determines the size of Einstein ring radius, and hence the image separation. However, $\langle\mu\rangle$ in such self-similar profiles is a constant, independent of absolute mass normalization.

Therefore galaxies must have changing logarithmic sur-

face mass density profiles in order to be able to reproduce the $\theta_{im}-z_s$ relation.

4 DISCUSSION

There are two interesting aspects in the observed distribution of image separations vs. source redshift. In this Letter I set out to explain one of these, the lack of high redshift wide separation lenses, i.e. the $\theta_{im}-z_s$ anticorrelation. It turns out that the model presented in Section 2 also naturally explains the other interesting feature of the $\theta_{im}-z_s$ plot, namely the existence of wide separation cases; there are 8 lensed QSOs with $\theta_{im} > 3''$. Most models currently found in the literature have trouble predicting a large population of wide separation lenses; for example MR93 predict the peak in θ_{im} distribution at $\lesssim 1''$, with vanishingly small number of cases above $3''$. So it has been argued that large θ_{im} cases are not due to isolated galaxies, but are the result of cluster-aided galaxy lensing. QSO 0957+561, with $6.1''$ between its two images, is adduced as supporting evidence. However, if cluster-aided galaxy lensing is the correct explanation, then wide separation lenses should be found at all redshifts, and not just at low z_s , as is currently the case (Figure 2). Furthermore, PG97 show that with the help of cluster lensing, image separation should *increase* with z_s . Since this is clearly not observed, cluster aided lensing is probably not important in general (0957 must be a special case), and the large number of wide separation lenses needs an explanation.

Let us derive the distribution of image separations as predicted by the model of Section 2. (I will use the ISC model because all the derivations required in this section can be carried out analytically with this model. However the general arguments presented here will also apply to the NFW profile.) So far only the dark matter halo properties have been discussed. These need to be related to the observable galaxy properties, like luminosity. I will adopt relations similar to those used in MR93 (their Section 2.2.1);

$$r_c \propto L^a, \quad M/L \propto L^b, \quad \text{hence} \quad \kappa_0 \propto L^{1-2a+b} \quad (4).$$

Optical effective radii of ellipticals are observed to scale as $L^{1.2}$ (Lauer 1985), and since it is commonly assumed that they are linearly proportional to the galaxies’ dark matter scale length, a is usually taken to be 1.2. From the observations of the fundamental plane of ellipticals (Kormendy & Djorgovski 1989), $b \approx 0.25$. Similar assumptions were made by Kochanek (1996). Parameter β of eq. (3) is $\beta = a/(1 - 2a + b)^\dagger$.

The frequency of multiply imaged QSOs as a function of image separation is given by,

$$\frac{dF}{d\langle\theta\rangle} = \frac{dN(L)}{dL} [r_c y_r(L)]^2 \frac{dL}{d\langle\theta(L)\rangle} \left(\frac{\langle\mu(L)\rangle}{f_{im}} \right)^s, \quad (5)$$

where $dN(L)/dL \propto L^{-1.2} e^{-L}$ is the Schechter luminosity function (Schechter 1976); L is in units of L_* , and I assume a constant slope of -1.2. The lensing cross section for a galaxy of luminosity L is given by the radial caustic in the source

[†] Note that MR93 and Kochanek (1996) assumed $a=1.2$, and $b = 0.25$, and hence effectively their $\beta = -1.04$, which would not reproduce the $\theta_{im}-z_s$ anticorrelation, see eq. (3).

plane, whose radius is $y_r(L) = (\kappa_0^{2/3} - 1)^{3/2}$. The image separation is approximately equal to the diameter of the tangential critical curve in the lens plane, $\langle \theta \rangle \approx 2r_c \sqrt{\kappa_0^2 - 1}$. Using eq. (4),

$$\frac{d\langle \theta(L) \rangle}{dL} = \frac{2r_{c,*} L^{a-1} (\kappa_0^2 [1 - a + b] - a)}{(\kappa_0^2 - 1)}. \quad (6)$$

Here, $r_{c,*}$ and $\kappa_{0,*}$ refer to the core radius and κ_0 of an L_* galaxy. I take $r_{c,*}$ to be $1.4h^{-1}\text{kpc}$, equal to the constant core radius derived in Section 2.2. The value of $\kappa_{0,*}$ is then calculated from $r_{c,*}$ and an assumed asymptotic line of sight velocity dispersion, $\sigma_* = 300\text{km s}^{-1}$; $\kappa_{0,*} = 5$. The last term in eq. (5) is the magnification bias.

The function $dF/d\langle \theta \rangle$ of eq. (5) is plotted in Figure 3, for a range of a corresponding to the allowable range of β , in eq. (3), $a=0.0, 0.2, 0.4, \text{ and } 0.6$; $b = 0.25$ was used throughout. The angular splitting by an L_* galaxy is denoted by an arrow. These predicted distributions apply to the source redshift range where the upper envelope, described by eq. (3) and plotted in Figure 2 does not cut in, i.e. for $z_s \lesssim 2.5$. The solid histogram is the observed distribution for the same source redshift cutoff. Even though the small number of currently observed lenses does not allow to make any precise conclusions, it is apparent that $a \sim 0.4$ reproduces the histogram quite well. The corresponding value of β is 0.9, which is perfectly consistent with the allowed range of β , -0.5 to 2 (see eq. [3]). Thus, $a \sim 0.4$ ($\beta \sim 0.9$) reproduces both the $\theta_{im}-z_s$ anticorrelation, and the observed frequency of wide separation lenses. In this scenario, the $\theta_{im} \sim 7''$ lenses are due to $\sim 2L_*$ galaxies, with a mass within $10h^{-1}\text{kpc}$ of $3.7 \cdot 10^{11} h^{-1} M_\odot$.

The major deviation of the present model from those found in the literature is in the value of a , the power law index relating the dark matter characteristic scale length of a galaxy to its luminosity. As mentioned earlier, a is usually assumed to be 1.2, while consistency with lensing observations in the framework of the present model implies $a \sim 0.4$.

5 CONCLUSIONS

If the observed distribution of image separation vs. source redshift of lensed QSOs is real and not a result of false lenses, like physical QSO pairs, then it has the following implications for galaxy dark matter halos: (i) galaxies must have changing logarithmic surface mass density profiles, with a ‘universal dark matter’ model being preferred over an isothermal sphere with a core, (ii) there must be a spread in galaxy properties, like the central surface mass density, (iii) the characteristic length scale of dark matter halos should scale with luminosity as L^a , where $a \sim 0.4$.

The corollary of the present model is that higher z_s multiply imaged QSOs are statistically more magnified, and are preferentially lensed by galaxies with lower central surface mass densities and intrinsic luminosities. These predictions can be tested if each lens case is modelled individually, which will become possible when the lensing galaxies of most multiply split QSOs are detected.

The strong dependence of the observed $\theta_{im}-z_s$ relation on galaxy properties means that it cannot be easily used as a test for the curvature of the Universe unless we know a lot more about the mass distribution of galaxies. Furthermore,

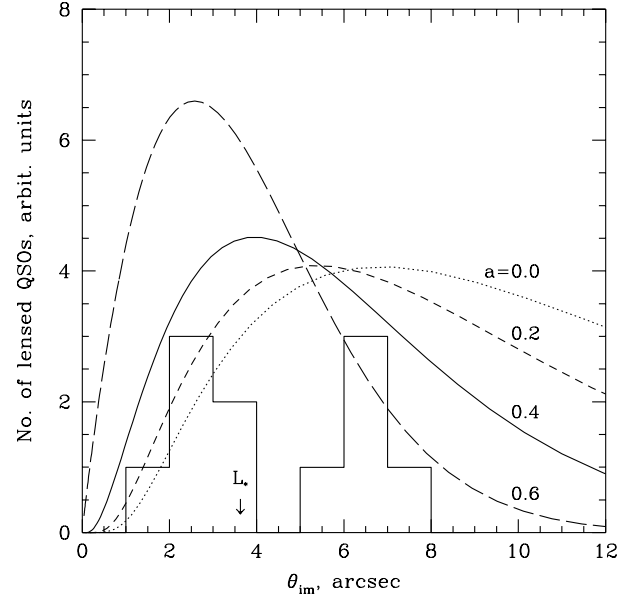


Figure 3. Predicted image separation distribution for lensed QSOs. The curves are labeled by parameter a , defined by $r_c \propto L^a$. Vertical normalization is arbitrary. The predictions are valid for z_s where the magnification bias effect, discussed in Section 2.2 and shown in Figure 2, does not impose an upper limit on θ_{im} of high- z_s lensed QSOs, i.e. for $z_s \lesssim 2.5$. Accordingly, the observed distribution to which the curves apply, is restricted to $z_s < 2.5$ and is shown as the solid histogram. Values of $a \sim 0.4$ seem to describe the observed distribution adequately. In these models image separation is a monotonically increasing function of galaxy luminosity; image separation produced by an L_* galaxy is indicated by an arrow.

because of the implications the present model has on the lensing properties of galaxy population, like the dependence of the predicted frequency of lensed QSOs on parameter a (see Figure 3), the current upper limits on Λ may have to be revised.

ACKNOWLEDGMENTS

I am grateful to Joachim Wambsgans for useful suggestions. I would like to acknowledge the support of PPARC fellowship at the Institute of Astronomy, Cambridge, UK.

REFERENCES

- Bartelmann, M. 1996, A&A, 313, 697
- Boyle, B. J., Shanks, T., & Peterson, B. A. 1990, MNRAS, 243, 1
- Evans, N. W., & Collett, J. L. 1997, Preprint, also available as astro-ph/9702085
- Fukugita, M., Futamase, T., Kasai, M., & Turner, E. L. 1992, ApJ, 393, 3
- Gott, R. J. III, Park, M.-G., & Lee, H. M. 1989, ApJ, 338, 1
- Hewett, P. C., Foltz, C. B., & Chaffee, F. H. 1993, ApJ 406, L43
- Kochanek, C. S., 1996. ApJ, 466, 638
- Kormendy, J. & Djorgovski, G. 1989, ARA&A, 27, 235
- Lauer, T. R. 1985, ApJ, 292, 104
- Lilly, S. J., Tresse, L., Hammer, F., Crampton, D., & Le Fevre, O. 1995, ApJ, 455, 108

- Park, M.-G., & Gott, R. J. III. 1997, Preprint, also available as astro-ph/9702173 (PG97)
- Maoz, D., & Rix, H.-W. 1993, ApJ, 416, 425 (MR93)
- Myers, S. T., *et al.* 1995, ApJ, 447, L5
- Navarro, J. F., Frenk, C. S., & White, S. D. M. 1995, MNRAS, 275, 720
- Navarro, J. F., Frenk, C. S., & White, S. D. M. 1996, ApJ, 462, 563
- Schechter, P. L., 1976. ApJ, 203, 297
- Schneider, P., Ehlers J. and Falco E. E. , 1992, Gravitational Lenses, Springer-Verlag Press
- Turner, E. L., 1990. ApJ, 365, L43
- Wallington, S., & Narayan, R. 1993, ApJ, 403, 517
- Williams, L. L. R., & Lewis, G. F. 1997, MNRAS, submitted